Broad-Band Emission Switch in Room Temperature Stable Hybrid Perovskite Polymorphs

Clémence Cazals, Nicolas Mercier, Magali Allain, Florian Massuyeau, Romain Gautier

RCover page

Broad-Band Emission Switch in Room Temperature Stable Hybrid Perovskite Polymorphs

Clémence Cazals,[a] Nicolas Mercier,[a] Magali Allain,[a] Florian Massuyeau[b] and Romain Gautier*[b]*

ABSTRACT – Low dimensional halide perovskites exhibiting broad band emission have attracted increasing attention owing to their potentiality in lighting applications. However, the relationships between the structure and luminescence properties remain unclear up to now. Here, we report a bromoplumbate organic-inorganic perovskite $(C3aH)_2PbBr_4$ ($C3aH^+$: 3-ammonium propionic acid cation) which exists as two polymorphs at room temperature (RT): the thermodynamically stable α-phase crystallizing in the $P2_1/n$ monoclinic space group, and the metastable β-phase crystallizing in the $P2_1/c$ monoclinic space group. α-$(C3aH)_2PbBr_4$ can be transformed into β-$(C3aH)_2PbBr_4$ by heating over 120 °C while the reversible transformation occurs upon cooling at very low temperature (100 K), or upon water or acetone atmosphere. Both polymorphs are built from <100> layered perovskites separated by the same $C3aH^+$ cations. No out-of-plane distortion of perovskite layers is observed in both structures but strong in-plane distortions with regular $PbBr_6$ octahedra are observed in the β-phase, whereas the α-phase exhibits strongly distorted $PbBr_6$ revealing the $6s^2$ lone pair stereo-activity. Interestingly, β-$(C3aH)_2PbBr_4$ exhibits a narrow emission band (blue emission), whereas α-$(C3aH)_2PbBr_4$ exhibits both narrow and broad bands (whitish emission). The existence of two perovskite polymorphs with different emission properties at a given temperature allows to establish structure-properties relationships, but also demonstrates that α-$(C3aH)_2PbBr_4$ can act as a room temperature luminescence switch material.

nicolas.mercier@univ-angers.fr - MOLTECH-Anjou, UMR-CNRS 6200, Université d'Angers - 2 Bd Lavoisier, 49045 Angers, France. Fax: +33.2.41.73.54.05; Tel: +33.2.41.73.50.83.

Broad-Band Emission Switch in Room Temperature Stable Hybrid Perovskite Polymorphs

Clémence Cazals,[a] Nicolas Mercier,[a] Magali Allain,[a] Florian Massuyeau[b] and Romain Gautier*[b]*

[a] MOLTECH-Anjou, UMR-CNRS 6200, Université d'Angers, 2 Bd Lavoisier, 49045 Angers, France. Fax: 33.(2).41.73.54.05; Tel: 33.(2).41.73.50.83.

[b] Nantes Université, CNRS, Institut des Matériaux de Nantes Jean Rouxel, IMN, F-44000 Nantes, France.

KEYWORDS (Word Style "BG_Keywords"). If you are submitting your paper to a journal that requires keywords, provide significant keywords to aid the reader in literature retrieval.

Lead Halide Perovskites (HP) have emerged as an important class of semiconductor materials. 2D perovskites consist of layers of organic cations separating perovskite sheets of PbX_6 octahedra extending in two directions of the space.[1-3] These layered perovskites, which are interesting materials for solar cell applications,[4-7] are also very promising for lighting applications.[8-10] Luminescence properties of A_2PbX_4 or $A'PbX_4$ layered perovskites (n= 1 member of the <100> series -B_nX_{3n+1} perovskite network-, X= Cl, Br, I; A^+ and A'^{2+} = organic cations) are well known since the 90's.[1,11-12] Due to electrical and dielectrical confinements within the inorganic layers, these layered materials exhibit strong exciton binding energies (up to 300 meV), which consequently lead to narrow emission owing to the recombination of the free exciton (FE) at room temperature.[13] First reported by Ishihara in the 90's,[14] and rediscovered recently,[15,16] some layered bromide or chloride perovskites can exhibit broad band (BB) emission in the whole visible range which has led to the emerging domain of halide layered perovskites for white light emission applications.[17-22] Karunadasa et al. have analyzed the structural features of n= 1 type perovskites, highlighting a correlation between the degree of out-of-plane distortion (tilt of octahedra resulting in X_{ap}-Pb-X_{ap} (ap: apical) lines which deviate from lines perpendicular to layers) and the origin of the emissions. They show that BB emitters are very often related to heavily distorted perovskite layers.[23,24] More recently, another descriptor has been proposed: the BB emission would be favored for HP based on perovskite layers for which four adjacent lead atoms define a rhomb.[25] However, many hybrid materials based on non-perovskite bromo- or chloroplumbate clusters (0D) or 1D networks have also been reported to exhibit broad band/white emission.[26-31] This shows that this property can be more generally associated to bromo- and chloroplumbate hybrid materials, also meaning that the specific descriptors for perovskite layers described above cannot be generalized to the whole family. A common descriptor should be related to the common structural feature of all these compounds: the PbX_6 octahedron. The octahedral deformation can be defined by several parameters including Δd related to bond distances, and σ^2 related to adjacent X-Pb-X angles. As soon as 2017, P. De Angelis et al. highlighted a relationship between the degree of octahedral distortion of some layered perovskites and the type of emission, narrow or broad band, showing that materials

based on highly distorted PbX_6 tend to give broad band emission.[32] The origin of broad band emission is commonly attributed to self-trapped excitons (STE)[8,23,24,33] generated upon excitation by the lattice deformability (intrinsic nature). The transfer from the HE state to the STE, and from STE to HE can occur through trapping and detrapping barriers, respectively. As a consequence the equilibrium between the HE and STE state emissions varies along with the temperature, the narrow emission being favoured at very low temperature (energy inferior to the trapping barrier) or at quite high temperature (energy superior to the detrapping barrier).[8,33] Moreover, the detrapping barrier decreases with the nature of halide, resulting in STE emission at RT for chloride or bromide based hybrids (quite high detrapping barriers) and narrow emission at RT for iodide based hybrids (quite small detrapping barrier).[33] Several studies have reported the effect of temperature on phase transitions and emission properties of specific HPs,[15-18,33-36] but, to the best of our knowledge, there is no report on the emission properties of two HP polymorphs which are stable in a common range of temperature. In this work, we report on a bromoplumbate layered perovskite $(C3aH)_2PbBr_4$ ($C3aH^+$: 3-ammonium propionic acid cation) belonging to the <100> series (n= 1 member) which exists as two polymorphs at room temperature (RT): the thermodynamically stable α-phase, and the metastable β-phase. The α-$(C3aH)_2PbBr_4$ is transformed into the β-phase by heating over 120 °C while the reversible transformation occurs upon cooling at very low temperature (100 K), and upon water or acetone atmosphere or upon strong grinding at RT. Interestingly, β-$(C3aH)_2PbBr_4$ exhibits a narrow emission band at 422 nm, typical of free exciton luminescence while α-$(C3aH)_2PbBr_4$ exhibits whitish emission composed of a quite broad excitonic peak at 438 nm with a tail extending down to about 650 nm. We will show that these specific emission properties can be related to structural features of both polymorphs. In particular, the specific organization of organic cations in the interlayer space leads for the β-phase to $PbBr_6$ units close to ideal octahedral geometry, and for the α-phase to $PbBr_6$ units strongly distorted revealing the $6s^2$ lone pair stereoactivity.

A slow evaporation from 70°C to room temperature of a HBr solution containing the two reagents $PbBr_2$ and $NH_2(CH_2)_2CO_2H$ (C3a, beta-alanine), leads to crystals of α-$(C3aH)_2PbBr_4$ (see SI for

experimental details). The Figure 1a shows the DSC curve of α-$(C3aH)_2PbBr_4$ in the 0°C-200°C temperature range. It clearly appears that an irreversible transition occurs at 104°C following by two reversible transformations. While the last one corresponds to a melting/crystallization process, the two first endothermic peaks are assigned to structural transitions, first from the α- form to the β- form and then from the β- form to an unknown γ- form. A slow heating of crystals of the α– phase up to 110 °C led to a single-crystal-to-single-crystal transformation into the β- phase, further allowing the crystal structure determination of β- at room temperature. These two consecutive phase transitions are confirmed by thermodiffractometry (Figure 1b). While increasing the temperature, a new set of XRD lines together with the disappearance of XRD lines corresponding to the α phase are observed around 104 °C corresponding to the first endothermic peak of the DSC curve. It appears that the new set of XRD lines perfectly correspond to XRD lines calculated for β-$(C3aH)_2PbBr_4$ from single crystal XRD data (Figure S1). The heating to 158 °C involves a shift of XRD lines and the appearance of a third set of XRD lines revealing the phase transformation from β- to γ-, while the cooling to room temperature confirms the reversibility of the β- to γ- transformation and the irreversibility of the β- to α- one. This means that α-$(C3aH)_2PbBr_4$ and β-$(C3aH)_2PbBr_4$ are two polymorphs which are stable at room temperature (under inert atmosphere for β). The metastable β-$(C3aH)_2PbBr_4$ phase can be transformed into the thermodynamically α-$(C3aH)_2PbBr_4$ phase through several process. After 30 min in a saturated atmosphere of water, a full conversion is observed (Figure S2). Interestingly, the unit cell of the β- phase ($V(\beta)= 885$ Å^3) is much larger than the one of the α- phase ($V(\alpha)/2= 818$ Å^3). Thus, one could expect a possible pressure induced β- to α- transformation. And, as expected, the α-$(C3aH)_2PbBr_4$ compound is partially recovered after a grinding of β-$(C3aH)_2PbBr_4$ and when β-$(C3aH)_2PbBr_4$ is immersed in liquid nitrogen for 15 minutes (Figure S2).

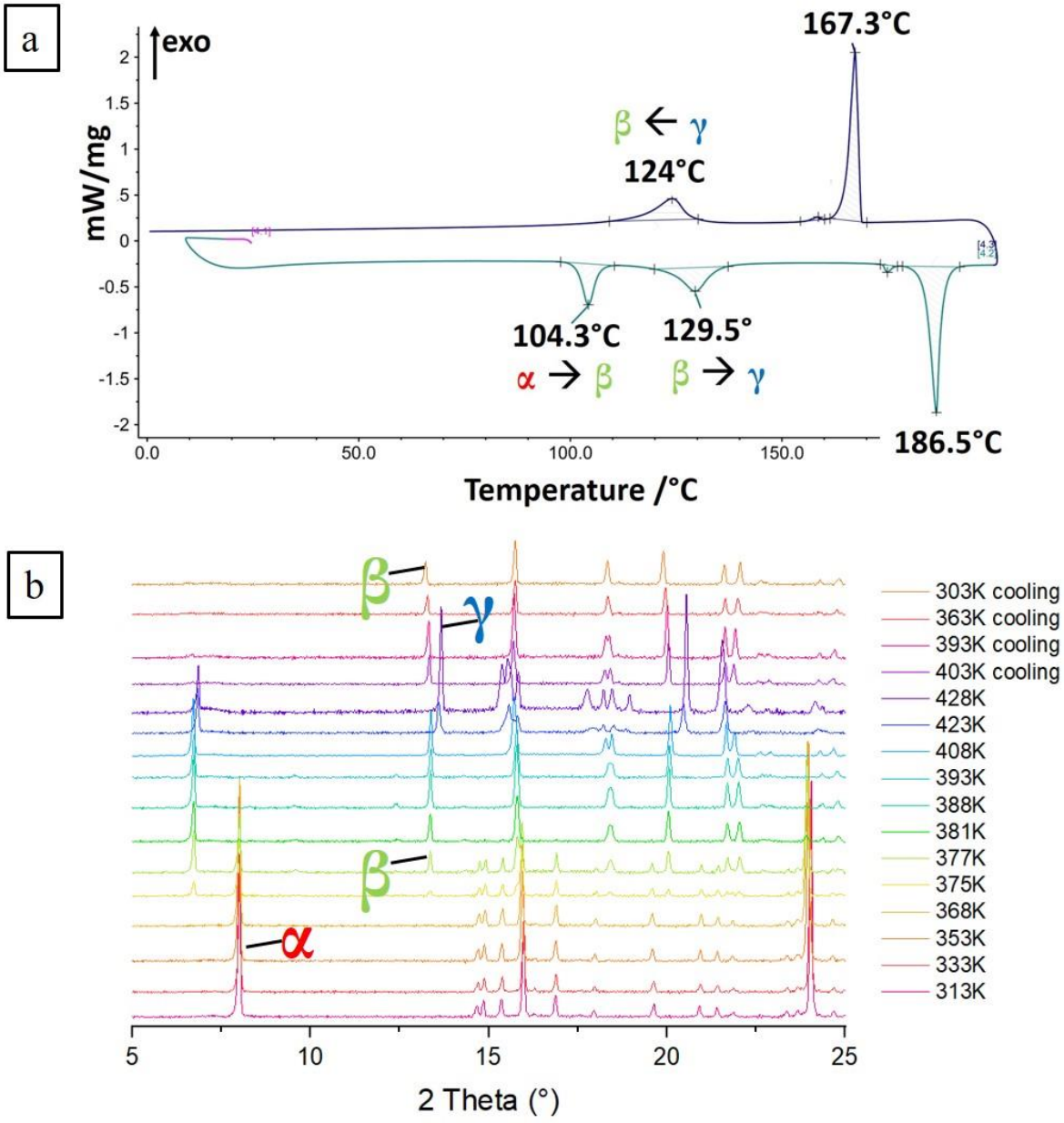

Figure 1. DSC curve of α-$(C3aH)_2PbBr_4$ in the 10°C-200°C temperature range, showing the α- to β-$(C3aH)_2PbBr_4$ transformation, and the reversible β- to γ- and melting transitions (a); Thermodiffractometry of a powder sample of α-$(C3aH)_2PbBr_4$ (nitrogen atmosphere) showing the α- to β- and β- to γ- transformations when T increases from 313 K to 428 K, and the γ- to β- transformation upon cooling (from 428 K to 303 K).

α-$(C3aH)_2PbBr_4$ has recently been reported to crystallize in the $P2_1/n$ monoclinic space group with two crystallographically independent organic molecules and one independent Pb^{2+} ion.[37] The new β-$(C3aH)_2PbBr_4$ crystallizes in the monoclinic $P2_1/c$ space group, the asymmetric unit containing one molecule and one Pb^{2+} ion located on a -1 site. A general view of the two structures is shown in Figure 2a and Figure 3a showing the very different organization of molecules in the interlayer space of these layered perovskites (<100> type). In the α- phase, molecules seem interpenetrated in order to fully fill the space, while in the β- phase, molecules are organized in dimers thanks to H bonds between the two CO_2H ends and seem to stand upright in the direction perpendicular to the perovskite layers. As a consequence, on the one hand, the interlayer space is shorter in the α- phase (≈ 11.15 Å) than in the β-phase (≈13.5 Å), and, on the other hand, the unit cell volume is lower in α- (V= 1635 $Å^3$) compared to β- (2 x V= 1770 $Å^3$). The Figures 2a and 3a also show that Pb^{2+} ions and equatorial bromides are roughly contained in planes and that very weak out-of-plane distortions of perovskite layers are observed (angles between Br_{ap}-Pb-Br_{ap} (ap: apical) lines and lines perpendicular to layers are estimated to 6.0° in α- and 6.4° in β-). As known, out-of-plane distortions, which consist of a tilt of octahedra with equatorial halides localized out of the average equatorial plane, are usually observed when only the NH_3^+ end of organic cations sit within the perovskite sheet. Here in both structures, at least two non-H atoms are localized in the perovskite sheet or at the limit of it, either a $CH_2NH_3^+$ fragment for all molecules in the β- structure and for one molecule in the α- structure, or a $CH_2CH_2NH_3^+$ fragment for the other molecule in the α-form.

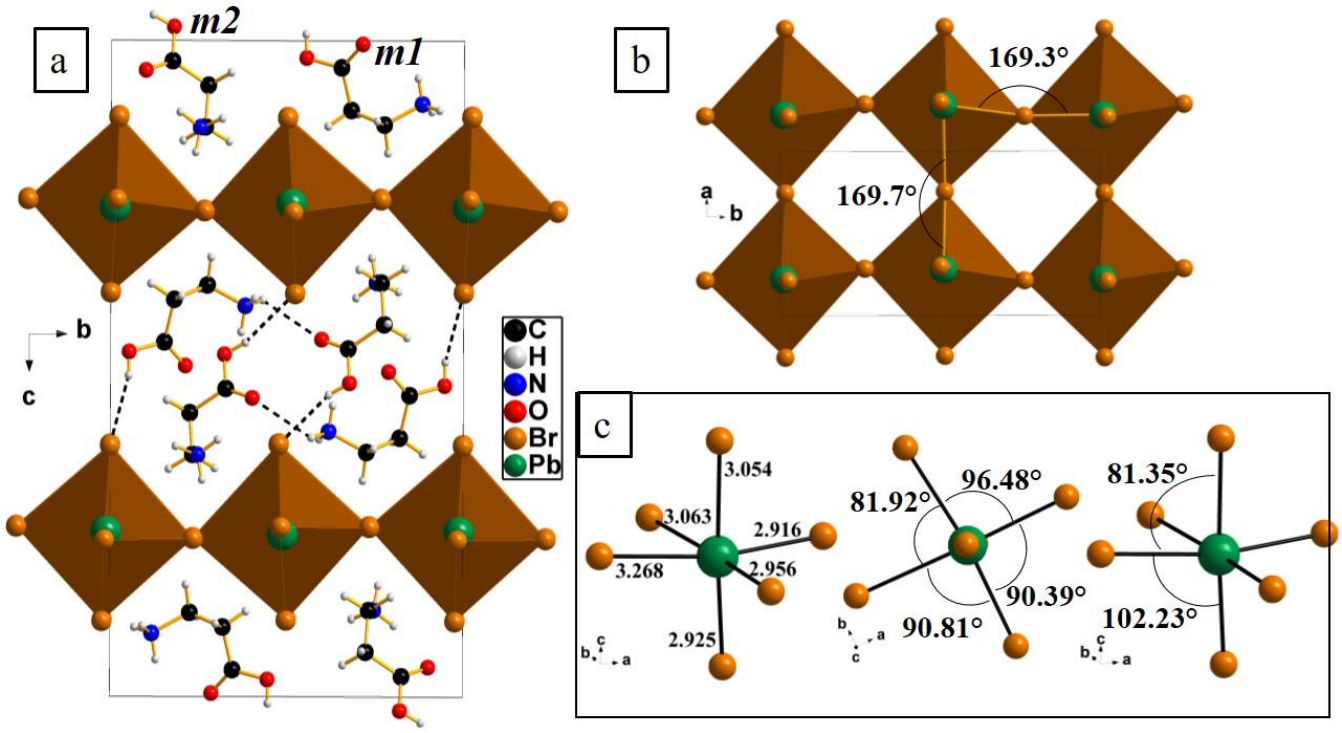

Figure 2. Room temperature crystal structure of α-$(C3aH)_2PbBr_4$: a) General view along *a* showing the organization of molecules in the interlayer space (dotted lines correspond to OH…Br -d < 2.50 Å-, the two independent molecules are named *m1* and *m2*) and NH…O (d < 2.53 Å) contacts; b) partial view of a perovskite layer highlighting in-plane distortions (Pb-Br-Pb bond angles are shown); c) bond distances and selected bond angles in the $PbBr_6$ octahedron.

The disposition of the $(CH_2)_2NH_3^+$ fragments of organic cations also influence the in-plane rotation of octahedra (known as in-plane distortions) of perovskites layers, resulting in Pb-Br_{eq}-Pb bond angles far from the ideal value of 180°. In the structure of the β- compound, there are quite strong in-plane distortions with Pb-Br_{eq}-Pb bond angles of 150.02° (Figure 3b). In contrast, weak in-plane distortions are present in the structure of the α- polymorph (Pb-Br_{eq}-Pb bond angles of 169.3° and 169.7°, Figure 2b). These weak distortions in α- can be explained by the special arrangement of molecules, which, on the one hand, have (molecules 1, *m1*) three non-H atoms in the perovskite sheet or at the limit of it, and, on the other end, have their NH_3^+ ends which are not (*m1*) or are partially (molecule 2, *m2*) involved in hydrogen bonding with equatorial bromides, thus limiting in-plane distortions. Indeed, as already

encountered in $(X(CH_2)_2NH_3)_2PbI_4$ (X= Cl, Br),[38] the NH_3^+ end of the C3aH$^+$ cation (*m1*, Figure 2a) is oriented towards the interlayer space to be in contact with an oxygen atom of a neighboring molecule (NH…O (d < 2.53 Å)). With respect to molecule 2, the C-N direction of the $CH_2NH_3^+$ being parallel to the perovskite plane, the NH_3^+ end preferentially makes H bonding with apical bromides. The other big difference between the two structures concerns the octahedral geometry, this structural feature being related to in-plane distortions. In the perovskite layer of the β- structure, octahedra rotate, but keep their nearly perfect octahedral geometry, in particular with all Pb-Br_{eq} bond distances close to 3.00 Å (Pb-Br_{eq}: 2.977 Å-3.008 Å range, Figure 3c), and all Br_{eq}-Pb-Br_{eq} bond angles close to 90 ° (Br_{eq}-Pb-Br_{eq} : 88.86°-91.14° range, Figure 3c). However, we can notice that Br_{ap}-Pb-Br_{eq} deviate from 90° by nearly 6° (Figure 3c), contributing to the rather high octahedral angle variance (σ^2 = 13.14 -σ^2= 1/11 $\Sigma(\alpha_i-90)^2$-). In the structure of α-, the rotation of octahedra is limited, but the $PbBr_6$ unit no longer retains octahedral geometry. Thus, short (2.916 Å) and long (3.268 Å) Pb-Br_{eq} bond distances are observed (the two others being 2.956 Å and 3.063 Å, Figure 2c), and both types of bond angles, Br_{eq}-Pb-Br_{eq} and Br_{ap}-Pb-Br_{eq}, deviate from 90° (81.92°-96.48° and 81.35-102.23°, respectively, Figure 2c) leading to a high octahedral angle variance (σ^2) of 31.8. All these structural features reveal the Pb^{2+} $6s^2$ lone pair stereo-activity in the structure of the α polymorph, while the lone pair can be considered as stereo-inactive in the structure of the β polymorph.

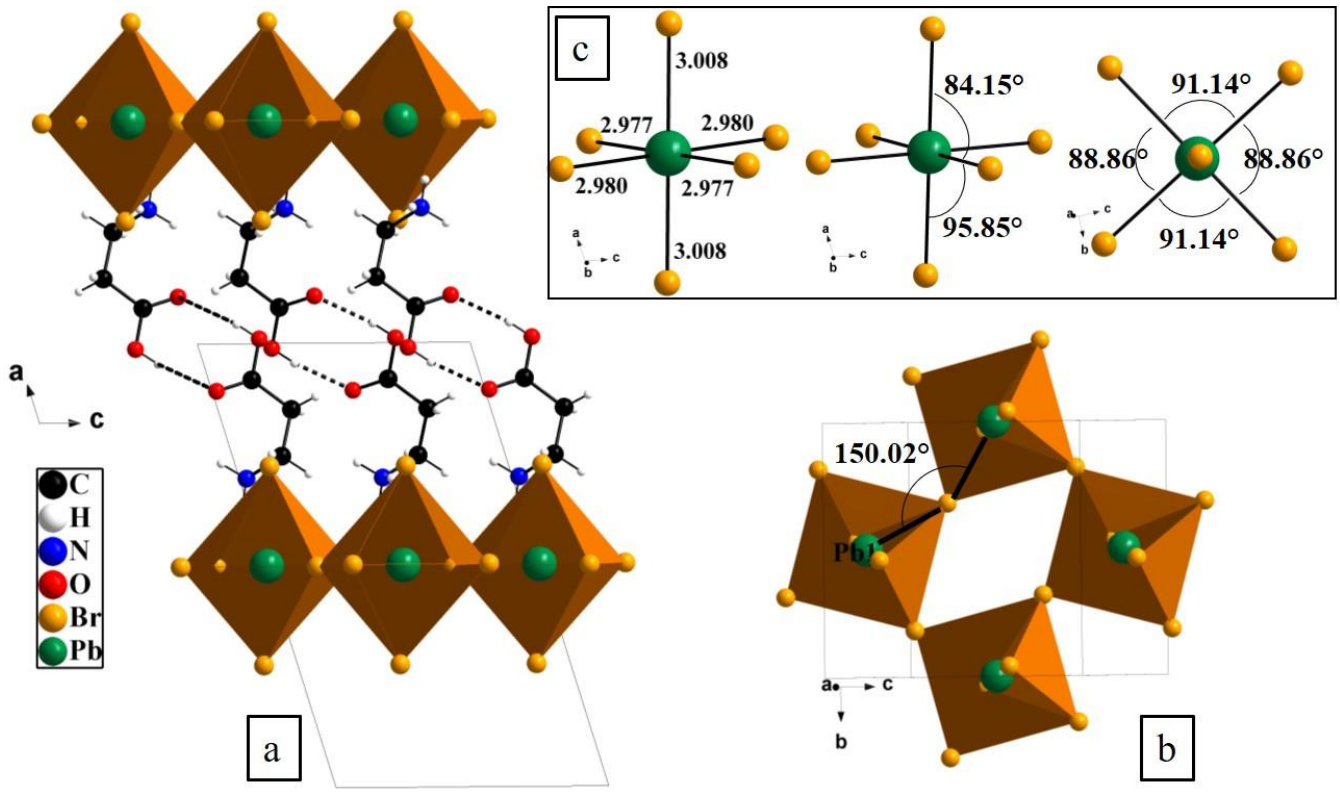

Figure 3. Room temperature crystal structure of β-$(C3aH)_2PbBr_4$ a) General view along *b* showing the organization of molecules in the interlayer space (dotted lines correspond to OH…O contacts -d < 2.12 Å); b) partial view of a perovskite layer highlighting in-plane distortions (Pb-Br-Pb bond angles are shown); c) bond distances and bond angles in the independent $PbBr_6$ octahedron.

The optical properties of both α-$(C3aH)_2PbBr_4$ and β-$(C3aH)_2PbBr_4$ (obtained by heating the α-compound and kept in inert atmosphere) have been investigated. The Figure 4a shows the absorption spectra where a similar main absorption band is observed at 384 nm indicating a similar optical band gap. At lower energy, the narrow peak is associated to the excitonic absorption. It is worth noting that the peak of the α- phase (416 nm) is red shifted compared to the one of the β- phase (406 nm), meaning that the binding exciton energy, which can be roughly estimated by the energy difference between the energies of the main absorption band and the excitonic peak, is higher in the α polymorph.

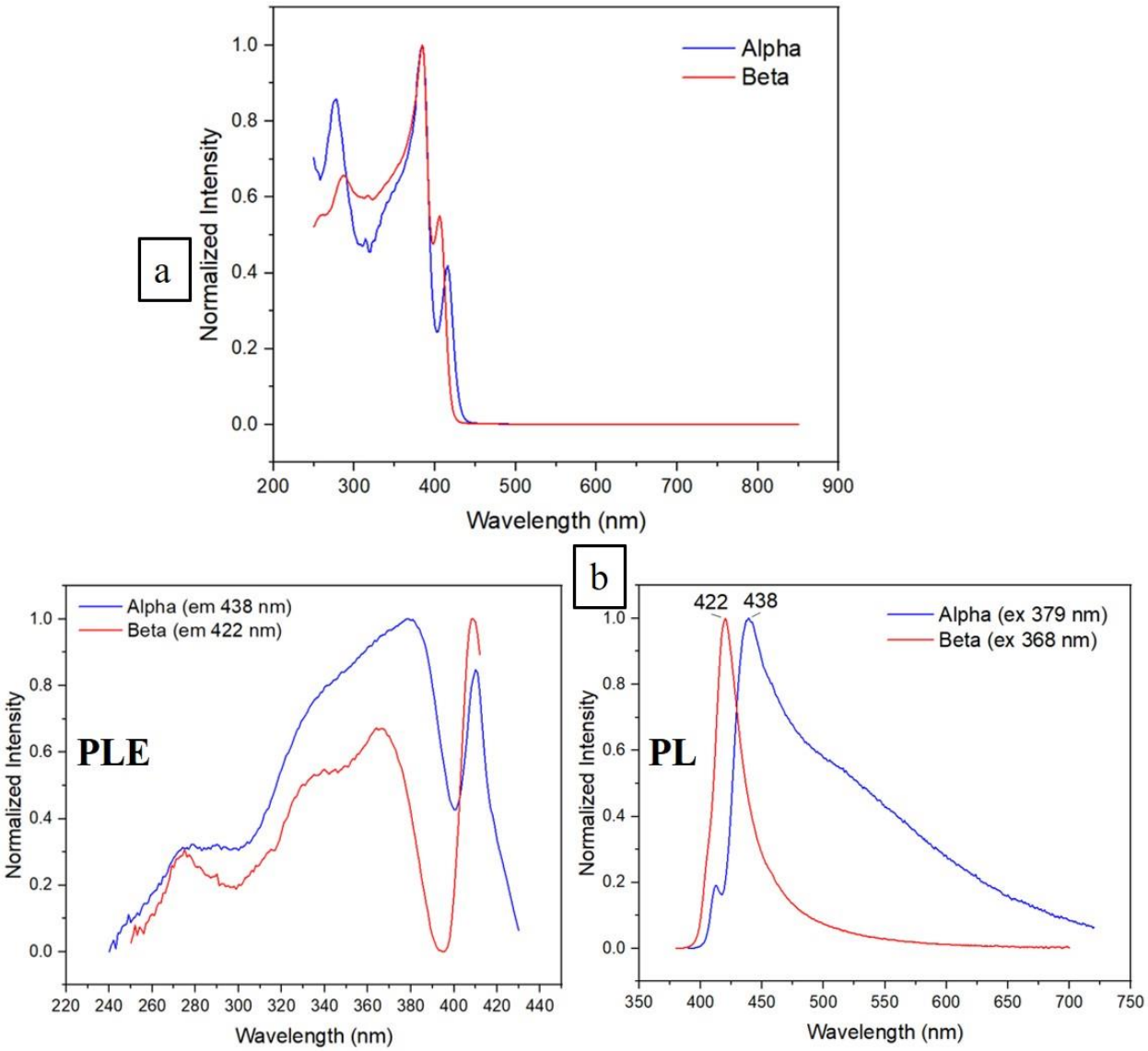

Figure 4. UV-Visible absorption spectra (a) and PL and PLE spectra of α-$(C3aH)_2PbBr_4$ and β-$(C3aH)_2PbBr_4$ (b).

The photoluminescence properties of both polymorphs are different (Figure 4b). Both photoluminescence spectra exhibit an excitonic peak (FE) at 422 nm (β-) and 438 nm (α-), the red shift for the α- polymorph being in good accordance with the observed red-shift of the excitonic absorption peak (Figure 4a). Interestingly, a double-peaked structure FE band is also observed for the α-form (Figure 4b). Such double-peaked structure of the FE emission was previously observed in other HP compounds and explained as the result of the self-absorption of the excitonic emission when the HP

shows small Stokes-shift as observed in our α compound.[39] In addition of these peaks, a broad band (STE) approximately centered at 525 nm is observed for the α- form. As a consequence, the emission of the α compound is whitish with CIE coordinates of (0.246, 0.268), while the emission of the β compound falls in the blue region (CIE coordinates of (0.171, 0.075), Figure S3). Moreover, if the broad band corresponds well to the main absorption band for α (380 nm / PLE vs 384 nm/Abs.), a blue shift is observed for β (366 nm / PLE vs 384 nm/Abs.). It appears that the different emission properties can be clearly related to the different structural features of these polymorphs which are mainly related to their octahedral geometry.

We carried out photoluminescence measurements depending on temperature. After cooling down a sample of α-$(C3aH)_2PbBr_4$ to low temperature, PL spectra were recorded upon heating, from 77K to 300 K (Figure 5a). The sample was then heated over 383 K in order to get the β- polymorph, followed by emission measurements upon cooling from 300 K to 77 K (Figure 5b, only PL at 300 K and 150 K are shown). As already observed, the cooling involves a blue shift of the excitonic peak, from 440 nm (300 K) to 411 nm (77 K) together with a decrease of its width, and a red shift of the broad band from 525 nm (300 K) to 625 nm (77 K) leading to a clear separation of both emissions at low temperature. We also observe that intensity ratio I(FE)/I(STE) increases when the temperature decreases meaning that the trapping barrier becomes difficult to cross upon cooling. As regards to the β polymorph, a blue shift of the exciton peak together with the decrease of the peak width is observed from 300 K to 150 K. At 77 K the PL spectrum (not shown) becomes complex due to the presence of both α and β polymorphs as a result of the β→α transformation at very low temperature. A great interest of this $(C3aH)_2PbBr_4$ halide perovskite existing as two polymorphs stable at room temperature and exhibiting different emission properties, is that the luminescence can be switched when one polymorph is transformed into the other. We carried out five "α→β and β→α" cycles, the first transformation being obtained by a fast heating of α at 110 °C, and the second one by exposing β to a saturated water atmosphere during 30 min. The PL spectra of α and β were collected for each cycle (Figure S4) showing the cyclability of the process. In

Figure 5c are reported the recorded intensities at λ= 500 nm illustrating the luminescence switch between the α phase (broad band emission in the whole visible range) and the β phase (narrow emission centered at 420 nm).

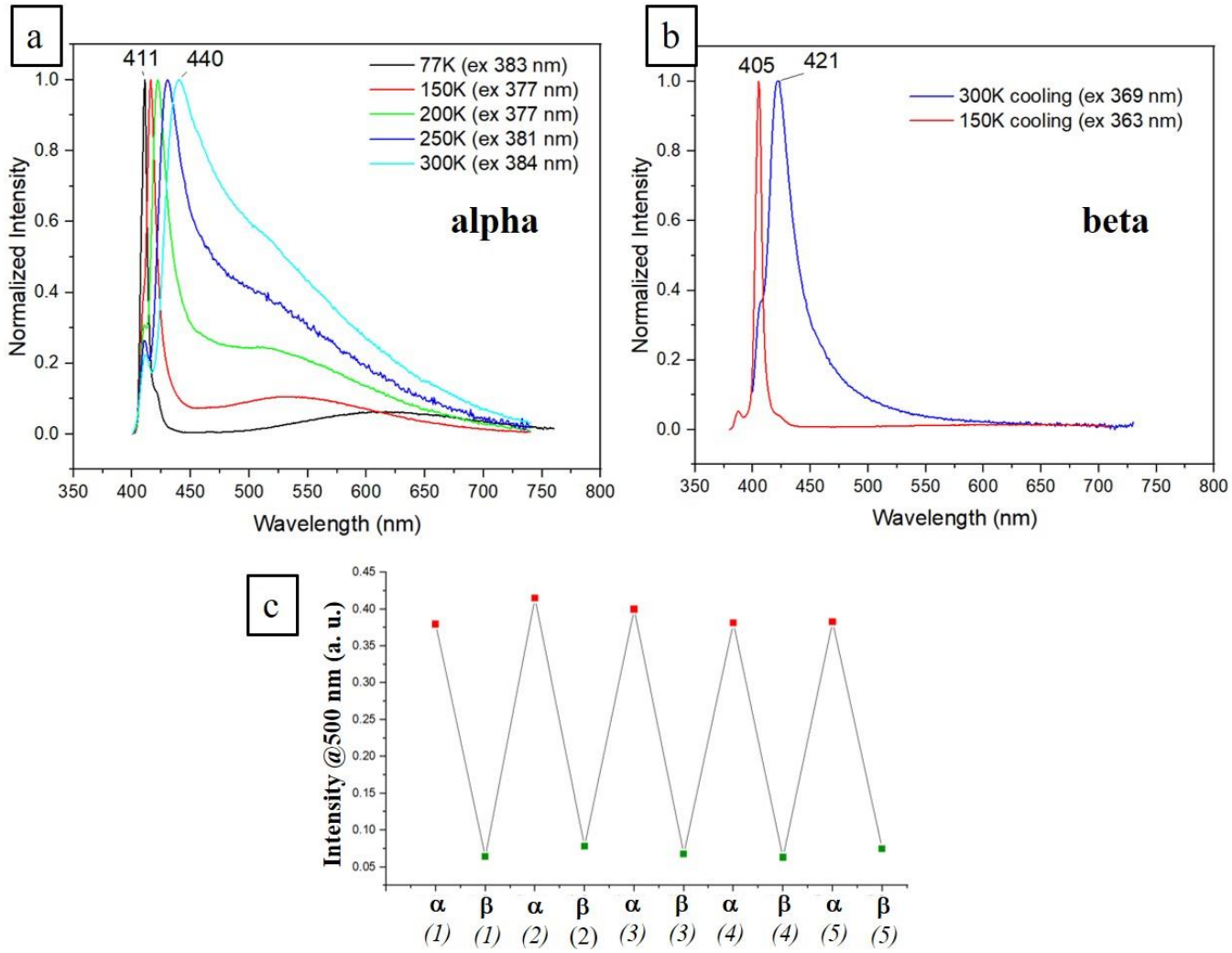

Figure 5. (a) PL spectra of a sample of α-$(C3aH)_2PbBr_4$ at different temperatures, from 77 K to 300 K; (b) PL of β-$(C3aH)_2PbBr_4$, obtained upon heating of the α- sample at 400 K, at 300 K and 150K; (c) luminescence intensity at λ= 500 nm (λ_{exc}= 365 nm, see spectra Figure S4) of α-$(C3aH)_2PbBr_4$ and β-$(C3aH)_2PbBr_4$ (right) along the 5 cycles (1 to 5) applied to an initial α sample (α to β transformation by heating a few minutes at 110°C, and β to α transformation upon water saturated atmosphere during 30 min).

In conclusion, we have presented here an unprecedented case of a bromoplumbate perovskite which exists as two polymorphs at room temperature: the thermodynamically stable α-$(C3aH)_2PbBr_4$ ($C3aH^+$: 3-ammonium propionic acid cation), and the metastable β-$(C3aH)_2PbBr_4$. We show that α-$(C3aH)_2PbBr_4$ can be transformed into the β-phase by heating over 110 °C while the reversible

transformation occurs upon cooling at very low temperature (100 K), or upon water or acetone atmosphere. While β-$(C3aH)_2PbBr_4$ exhibits a narrow emission band (blue emission), α-$(C3aH)_2PbBr_4$ exhibits both narrow and broad bands resulting in whitish emission. It appears that these different emission properties can be clearly related to the different structural features of these polymorphs which are mainly related to their octahedral geometry: distorted $PbBr_6$ unit revealing the $6s^2$ lone pair stereoactivity in α *vs* a quite perfect $PbBr_6$ octahedral geometry in β. We also show that the luminescence properties of α can be tuned according to the temperature as the FE peak is blue-shifted and the STE band is red-shifted. Finally, taking advantage of the existence of these two room temperature stable polymorphs with different emission properties, we demonstrated that $(C3aH)_2PbBr_4$ can be considered as a switchable luminescent material.

ASSOCIATED CONTENT

Supporting Information. Details of synthesis procedures. Complete single crystal X-ray data. X-ray Powder Diffraction patterns. CIE coordinates graphs. This information is available free of charge via the Internet at http://pubs.acs.org/

AUTHOR INFORMATION

Corresponding Author

*nicolas.mercier@univ-angers.fr, romain.gautier@cnrs-imn.fr

Author Contributions

The manuscript was written through contributions of all authors. All authors have contributed equally and have given approval to the final version of the manuscript.

ACKNOWLEDGMENT

C. Cazals thanks the LUMOMAT program for a phD grant.

REFERENCES

(1) Mitzi D. B., Prog. Inorg. Chem. (Ed. Karlin, K. D.), John Wiley & Sons, Inc.: Hoboken, NJ, USA, **1999**; pp 1−121.

(2) Saparov, B.; Mitzi, D. B. Organic-Inorganic Perovskites: Structural Versatility for Functional Materials Design. *Chem. Rev.* **2016**, *116*, 4558−4596.

(3) Mercier, N. Hybrid Halide Perovskites: Discussions on Terminology and Materials. *Angew. Chemie Int. Ed.* **2019**, *58*, 17912-17917

(4) Ren, H.; Yu, S.; Chao, L.; Xia, Y.; Sun, Y.; Zuo, S.; Li, F.; Niu, T.; Yang, Y.; Ju, H.; Li, B.; Du, H.; Gao, X.; Zhang, J.; Wang, J.; Zhang, L.; Chen, Y.; Huang, W. Efficient and stable Ruddlesden–Popper perovskite solar cell with tailored interlayer molecular interaction. *Nat. Photonics* **2020**, *14*, 154−163.

(5) Liang, C.; Gu, H.; Xia, Y.; Wang, Z.; Liu, X.; Xia, J.; Zuo, S.; Hu, Y.; Gao, X.; Hui, W.; Chao, L.; Niu, T.; Fang, M.; Lu, H.; Dong, H.; Yu, H.; Chen, S.; Ran, X.; Song, L.; Li, B.; Zhang, J.; Peng, Y.; Shao, G.; Wang, J.; Chen, Y.; Xing, G.; Huang, W. Two-dimensional Ruddlesden–Popper layered perovskite solar cells based on phase-pure thin films. *Nat. Energy* **2021**, *6*, 38-45

(6) Li, X.; Hoffman, J. M.; Kanatzidis, M. G. The 2D Halide Perovskite Rulebook: How the Spacer Influences Everything from the Structure to Optoelectronic Device Efficiency. *Chem. Rev.* **2021**, *121*, 2230–2291.

(7) Sidhik, S.; Wang, Y.; De Siena, M.; Asadpour, R.; Torma, A. J.; Terlier, T.; Ho, K.; Li, W.; Puthirath, A. B.; Shuai, X.; Agrawal, A.; Traore, B.; Jones, M.; Giridharagopal, R.; Ajayan, P. M.; Strzalka, J.; Ginger, D. S.; Katan, C.; Alam, M. A.; Even, J.; Kanatzidis, M. G.; Mohite, A. D. Deterministic Fabrication of 3D/2D Perovskite Bilayer Stacks for Durable and Efficient Solar Cells. *Science* **2022**, *377* (6613), 1425–1430

(8) Smith, M. D.; Connor, B. A.; Karunadasa, H. I. Tuning the luminescence of layered halide perovskites. *Chem. Rev.* **2019**, *119*, 3104-3139.

(9) Cortecchia, D.; Yin, J.; Petrozza, A.; Soci, C. White light emission in low-dimensional perovskites. *J. Mater. Chem. C* **2019**, *7*, 4956-4969.

(10) Mao, L.; Guo, P.; Kepenekian, M.; Hadar, I.; Katan, C.; Even, J.; Schaller, R. D.; Stoumpos, C. C.; Kanatzidis, M. G. Structural Diversity in White-Light-Emitting Hybrid Lead Bromide Perovskites. *J. Am. Chem. Soc.* **2018**, *140*, 13078−13088.

(11) Papavassiliou, G. C. Three- and low-dimensional inorganic semiconductors. *Prog Solid State Chem*. **1997**, *25*, 125-270.

(12) Era, M.; Morimoto, S.; Tsutsui, T.; Saito, S. Organic-inorganic heterostructure electroluminescent device using a layered perovskite semiconductor $(C_6H_5C_2H_4NH_3)_2PbI_4$. *Appl. Phys. Lett*. **1994**, *65*, 676– 678

(13) Katan, C.; Mercier, N.; Even, J. Quantum and Dielectric Confinement Effects in Lower-Dimensional Hybrid Perovskite Semiconductors. *Chem. Rev.* **2019**, *119*, 3140–3192

(14) Nagami, A. ; Okamura, K.; Ishihara, T. Optical properties of a quantum wire crystal, $C_5H_{10}NH_2PbI_3$. *Phys. B* **1996**, *227*, 346-348.

(15) Dohner, E. R.; Hoke, E. T.; Karunadasa, H. I. Self-Assembly of Broadband White-Light Emitters. *J. Am. Chem. Soc.* **2014**, *136*, 1718-1721.

(16) Dohner, E. R.; Jaffe, A.; Bradshaw, L. R.; Karunadasa, H. I. Intrinsic white-Light Emission from Layered Hybrid Perovskites. *J. Am. Chem. Soc.* **2014**, *136*, 13154-13157.

(17) Yangui, A.; Garrot, D.; Lauret, J. S.; Lusson, A.; Bouchez, G.; Deleporte, E.; Pillet, S.; Bendeif, E. E.; Castro, M.; Triki, S.; Abid, Y.; Boukheddaden, K. Optical Investigation of Broadband White-Light Emission in Self-Assembled Organic-Inorganic Perovskite (C6H11NH3)(2)PbBr4. *J Phys Chem C* **2015**, *119*, 23638-23647

(18) Yang, S.; Wu, D.; Gong, W.; Huang, Q.; Zhen, H.; Ling, Q.; Lin, Z. Highly efficient room-temperature phosphorescence and afterglow luminescence from common organic fluorophores in 2D hybrid perovskites. *Chem. Sci.* **2018**, *9*, 8975-8981.

(19) Zhou, G.; Li, M.; Zhao, J.; Molokeev, M. S.; Xia, Z. Single-Component White-Light Emission in 2D Hybrid Perovskites with Hybridized Halogen Atoms. *Adv. Opt. Mater.* **2019**, *7*, 1901335

(20) Pareja-Rivera, C.; Morán-Muñoz, J. A.; Gómora-Figueroa, A. P.; Jancik, V.; Vargas, B.; Rodríguez-Hernández, J.; Solis-Ibarra, D. Optimizing Broadband Emission in 2D Halide Perovskites. *Chem. Mater.* **2022**, *34*, 9344-9349.

(21) Jung, M.-H. White-Light Emission from the Structural Distortion Induced by Control of Halide Composition of Two-Dimensional Perovskites ((C6H5CH2NH3)2PbBr4–xClx). *Inorg. Chem.* **2019**, *58*, 6748-6757

(22) Hleli, F.; Mercier, N.; Ben Haj Salah, M.; Allain, M.; Travers, T.; Gindre, D.; Zouari, N.; Botta, C. Morphology and Temperature Dependence of a Dual Excitonic Emissive 2D Bromoplumbate Hybrid Perovskite: The Key Role of Crystal Edges. *J . Mater. Chem. C* **2022**, *10*, 10284-10291.

(23) Smith, M. D.; Jaffe, A.; Dohner, E. R.; Lindenberg, A. M.; Karunadasa, H. I. Structural origins of broadband emission from layered Pb–Br hybrid perovskites. *Chem. Sci.* **2017,** *8*, 4497-4504

(24) Smith, M. D.; Karunadasa, H. I. White-Light Emission from Layered Halide Perovskites. *Accounts of Chemical Research* **2018**, *51*, 619-627

(25) Han, X.-B.; Jing, C.-Q.; Zu, H.-Y.; Zhang, W. Structural Descriptors to Correlate Pb Ion Displacement and Broadband Emission in 2D Halide Perovskites. *J. Am. Chem. Soc.* **2022**, *144*, 18595-18606.

(26) Yuan, Z.; Zhou, C. K.; Tian, Y.; Shu, Y.; Messier, J.; Wang, J. C.; van de Burgt, L. J.; Kountouriotis, K.; Xin, Y.; Holt, E.; Schanze, K.; Clark, R.; Siegrist T.; Ma, B. W. One-dimensional organic lead halide perovskites with efficient bluish white-light emission. *Nature Communications*, 2017, **8**, 14051.

(27) Ben Hah Salah, M.; Mercier, N.; Allain, M.; Zouari, N.; Botta, C. Dual Phosphorescence from the organic and inorganic moieties of 1D Hybrid Perovskites of the $Pb_{n'}Br_{4n'+2}$ Series (n' = 2, 3, 4, 5). *J. Mater. Chem. C* **2019**, *7*, 4424-4433

(28) Q. Yao, J. Zhang, K. Wang, L. Jing, X. Cheng, C. Shang, J. Ding, W. Zhang, H. Sun and T. Zhou, *J. Mater. Chem. C*, 2021, **9**, 7374-7383

(29) Barkaoui, H.; Abid, H.; Yangui, A.; Triki, S.; Boukheddaden, K.; Abid, Y. Yellowish White-Light Emission Involving Resonant Energy Transfer in a New One-Dimensional Hybrid Material: $(C_9H_{10}N_2)PbCl_4$. *J. Phys. Chem. C* **2018**, *122*, 24253-24261

(30) Peng, Y; Yao, Y. ; Li, L. ; Wu, Z. ; Wang, S. ; Luo, J. White-light emission in a chiral one-dimensional organic–inorganic hybrid perovskite. *J. Mater Chem C* **2018**, *6*, 6033-6037.

(31) Cheng, X.; Yue, S.; Chen, R.; Yin, J.; Cui, B.-B. White Light-Emitting Diodes Based on One-Dimensional Organic–Inorganic Hybrid Metal Chloride with Dual Emission. *Inorg. Chem.* **2022**, *61*, 15475-15483.

(32) Cortecchia, D.; Neutzner, S.; Kandada, A. R. S.; Mosconi, E.; Meggiolaro, D.; De Angelis, P.; Soci, C.; Petrozza, A. Broadband Emission in Two-Dimensional Hybrid Perovskites: The Role of Structural Deformation. *J. Am. Chem. Soc.* **2017**, *139*, 39-42.

(33) Gautier, R.; Paris, M.; Massuyeau, F. Exciton-self-trapping in hybrid lead halides: Role of halogen. *J. Am. Chem. Soc.* **2019**, *141*, 12619-12623.

(34) Hu, T.; Smith, M. D.; Dohner, E. R.; Sher, M.-J.; Wu, X.; Trinh, M. T.; Fisher, A.; Corbett, J.; Zhu, X.-Y.; Karunadasa, H. I.; Lindenberg, A. M. Mechanism for Broadband White-Light Emission from Two-Dimensional (110) Hybrid Perovskites. *J. Phys. Chem. Lett.* **2016**, *7*, 2258-2263.

(35) Li, X.; Guo, P.; Kepenekian, M.; Hadar, I.; Katan, C.; Even, J.; Stoumpos, C. C.; Schaller, R. D.; Kanatzidis, M. G. Small Cyclic Diammonium Cation Templated (110)-Oriented 2D Halide (X = I, Br, Cl) Perovskites with White-Light Emission. *Chem. Mater.* **2019**, *31*, 3582-3290.

(36) Thirumal, K.; Chong, W. K.; Xie, W.; Ganguly, R.; Muduli, S. K.; Sherburne, M.; Asta, M.; Mhaisalkar, S.; Sum, T. C.; Soo, H. S.; Mathews, N. Morphology-Independent Stable White-Light Emission from Self-Assembled Two-Dimensional Perovskites Driven by Strong Exciton–Phonon Coupling to the Organic Framework. *Chem. Mater.* **2017**, *29*, 3947-3953

(37) Zu, H.-Y.; Fan, C.-C.; Liu C.-D.; Jing, C.-Q.; Chai, C.-Y.; Liang, B.-D.; Han X.-B.; Zhang, W. Establishing a Relationship between the Bandgap and the Structure in 2D Lead Halide Perovskite Semiconductors. *Chem. Mater.* **2023**, *35*, 5854-5863.

(38) Sourisseau, S.; Louvain, N.; Bi, W.; Mercier, N.; Rondeau, D.; Boucher, F.; Buzaré, J.-Y.; Legein, C. Reduced Band Gap Hybrid Perovskites Resulting from Combined Hydrogen and Halogen Bonding at the Organic−Inorganic Interface. *Chem. Mater.* **2007**, *19*, 600–607

(39) Febriansyah, B.; Borzda, T.; Cortecchia, D.; Neutzner, S.; Folpini, G.; Ming Koh, T.; Li, Y.; Mathews, N.; Petrozza, A.; England, J. Metal Coordination Sphere Deformation Induced Highly Stokes-Shifted, Ultra Broadband Emission in 2D Hybrid Lead-BromidePerovskites and Investigation of Its Origin. *Angew. Chem. Int. Ed.* **2020**, *59*, 10791-10796.

For Table of Contents Use Only

Manuscript title

Broad-Band Emission Switch in Room Temperature Stable Hybrid Perovskite Polymorphs

Authors

Clémence Cazals, Nicolas Mercier,* Magali Allain, Florian Massuyeau and Romain Gautier*

Synopsis

A bromoplumbate organic-inorganic perovskite $(C3aH)_2PbBr_4$ ($C3aH^+$: 3-ammonium propionic acid cation) exists as two polymorphs which are stable at room temperature (RT): the thermodynamically stable α-phase exhibiting both narrow and broad band emission, and the metastable β-phase exhibiting a narrow emission band, meaning that this compound can act as luminescence switchable material. The specific luminescent properties of both polymorphs are related to the stereo-activity (α-) or stereo-inactivity (β) of the Pb^{2+} $6s^2$ lone pair.

TOC graphic